Journal of Physics: Conference Series **493** (2014) 012028 doi:10.1088/1742-6596/493/1/012028

Lithographically-fabricated channel arrays for confocal x-ray fluorescence microscopy and XAFS

Arthur R. Woll[1], David Agyeman-Budu[2], Sanjukta Choudhury[3], Ian Coulthard[4], Adam C. Finnefrock[5], Robert Gordon[6], Emil Hallin[4], and Jennifer Mass[7]

[1] Cornell High Energy Synchrotron Source, Cornell University, Ithaca, NY 14853, USA
[2] Dept. of Materials Science, Cornell University, Ithaca, NY 14853, USA
[3] Geol. Sciences, Univ. of Saskatchewan, 114 Science Place, Saskatoon SK S7N 5E2 Canada
[4] Canadian Light Source, 44 Innovation Blvd, Saskatoon, SK S7N 2V3, Canada
[5] Merck Research Laboratories, 770 Sumneytown Pike, West Point, PA 19486, USA
[6] PNCSRF, APS Sector 20, 9700 S. Cass Ave. 435E, Argonne, IL 60439 USA
[7] Winterthur Museum, Winterthur, DE, 19735, USA

E-mail: `arthurwoll@cornell.edu`

Abstract. Confocal X-ray Fluorescence Microscopy (CXRF) employs overlapping focal regions of two x-ray optics—a condenser and collector—to directly probe a 3D volume. The minimum-achievable size of this probe volume is limited by the collector, for which polycapillaries are generally the optic of choice. Recently, we demonstrated an alternative collection optic for CXRF, consisting of an array of micron-scale collimating channels, etched in silicon, and arranged like spokes of a wheel directed towards a single source position. The optic, while successful, had a working distance of only 0.2 mm and exhibited relatively low total collection efficiency, limiting its practical application. Here, we describe a new design in which the collimating channels are formed by a staggered array of pillars whose side-walls taper away from the channel axis. This approach improves both collection efficiency and working distance, while maintaining excellent spatial resolution. We illustrate these improvements with confocal XRF data obtained at the Cornell High Energy Synchrotron Source (CHESS) and the Advanced Photon Source (APS) beamline 20-ID-B.

1. Introduction

Over the past 10 years, confocal x-ray fluorescence microscopy (CXRF) has become an increasingly common approach to the problem of obtaining elemental composition distributions in three dimensions. As described in several recent reviews [1], it has been demonstrated at numerous synchrotrons worldwide as well as with lab-based sources, and applied to a wide variety of applications. Recently, we demonstrated the first use of lithographically-etched channels in silicon as a collection optic for CXRF [2]. In this approach, the collection optic determines one of the three dimensions of the confocal probe volume, whereas the remaining two are defined by the incident beam. Ref. [2] demonstrates an order-of-magnitude improvement in resolution when compared with state-of-the-art demonstrations of CXRF, virtually all of which use polycapillaries for collection. However, the optics employed in Ref. [2] have limited practical appeal, exhibiting relatively poor collection efficiency compared to polycapillaries and a very small working distance, approximately 0.2 mm. The collection efficiency of these optics,

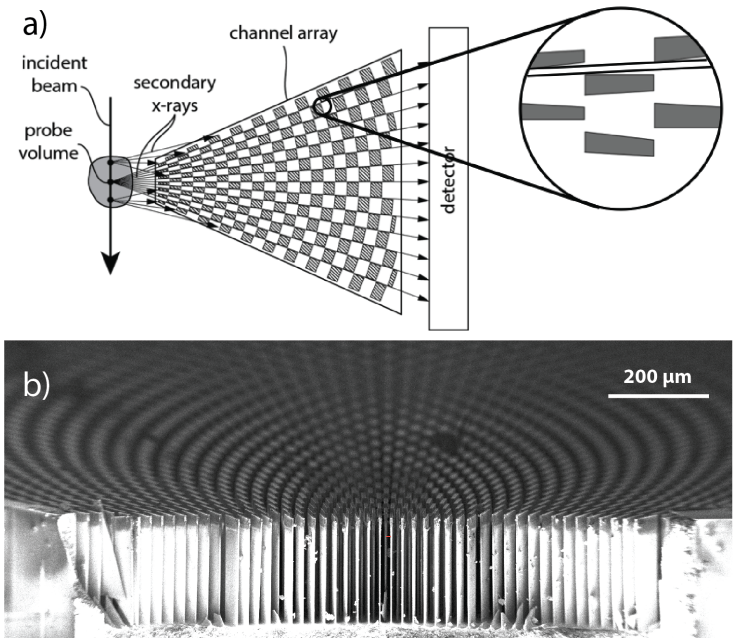

Figure 1. (a) Schematic illustration of CXRF configuration using collimating channels that are formed from a set of staggered, absorbing pillars. The inset illustrates that the pillar edges are tapered away from the axis of each channel to absorb reflected photons. (b) Scanning electron micrograph of a channel array formed by an arrangement of staggered, tapered pillars etched into a silicon substrate. The optic shown has an effective channel width of ≈2.2 μm, but the effective channel depth is over 200 μm.

defined [2] as the fraction of fluorescent photons emitted from a point source captured and transmitted by the optic, was limited by the channel depth, which varied from 30-50 μm for channel widths of 1-5 μm. The small working distance of these optics was necessitated by the large, diffuse reflectivity of the channels. As a result, the collimating power or angular selectivity δ of the channels was much larger than the designed value, w/l, the ratio of the channel width w and length l.[1] Because the spatial resolution r of the channel array is approximately $w + \delta f$, (where f is the working distance from the sample to optic), large δ requires small f in order to achieve small values of r.

Here, we report fabrication of an improved channel array design, illustrated in figure 1a, that addresses both of these limitations. A key feature of this approach is that channels are effectively formed by a series of staggered pillars. This arrangement increases the distance between features without increasing the channel width, allowing much greater etch depth. Figure 1b shows a scanning electron micrograph (SEM) of an optic fabricated with such a design, illustrating effective channel depths upwards of 200 μm. The optic in figure 1b was designed with 2 μm channels, so that the effective aspect ratio of channels is approximately 100:1. The second key feature of this design, indicated in the inset of figure 1a, is that the pillars forming each channel are tapered away from the channel axis. Such tapering successfully reduces the angular acceptance of the channels, thus allowing an increase in working distance while maintaing good spatial resolution. Below, we present an overview of recent results obtained at both CHESS and APS 20-ID-B using channel arrays that incorporate these ideas.

[1] Note that this definition of δ is a factor of 2 smaller than that defined in Ref. [2], resulting in a compensating change in the definition of channel resolution r.

2. Results

Based on the principles described above, new optics were designed, fabricated and characterized using techniques described in Ref. [2]. The angular selectivity of the channels is measured by directing a well-collimated incident beam through a single channel, then rotating the optic about its focal point and measuring the transmitted intensity. Two optics representing the new design, having channel dimensions of 1 μm $\times$ 4 mm and 7 μm $\times$ 4 mm, were found to have angular selectivities δ of 2.2 and 3.3 mrad, respectively, at 10 keV. These values represent a factor-of-two or better reduction compared to the straight channels described in Ref. [2], and are sufficient to allow modest increases in f without greatly increasing r, as shown below. Nevertheless, they are significantly larger than their ideal, geometric collimation w/l, 0.25 and 1.75 mrad. Comparison with ray-tracing simulations suggest that the broadening of δ for these channels is induced by refraction at the front edges of the tapered pillars (see Fig. 1a).

We have employed these optics for confocal XRF at both the G1 station at CHESS and APS station 20 ID B, for both XRF mapping and confocal XAFS [3, 4]. Tests at CHESS employing the 7 μm $\times$ 4 mm channel array demonstrate that the increased channel depth of these arrays gives rise to a commensurate increase in collection efficiency. To measure this efficiency, we direct a focused incident x-ray beam, approximately 3μm in diameter, onto a metal film, approximately 200-nm thick, such that the illuminated area of the film acts as a point source of x-ray fluorescence. By comparing the fluorescence intensity from this source measured with and without our optic in place, the collection efficiency may be determined as a fraction of 4π. For this array, we obtain a value of 0.14% near 9 keV – a factor of 10 greater than that reported previously, and nearly equivalent to that of a polycapillary measured with an otherwise identical setup.

An additional, critical test of the new design is whether comparable resolution to that reported in Ref. [2] could be achieved with a larger working distance f. This test was carried out at APS 20-ID-B, for which a KB mirror pair was used to focus the incident beam to approximately 1.5 μm (HZ) $\times$ 2μm (VT). The 1 μm $\times$4 mm channel array, with a working distance of 0.5 mm, was employed. The depth resolution d_R [2], was measured by scanning the surface of NIST SRM 1834 through the confocal volume and fitting to the error function, modified to include attenuation [5]. An example of such a scan and fit is shown as the inset to figure 2. The depth resolution corresponds to the sharpness of the left-hand edge of this curve. Figure 2 shows the values of d_R obtained for different emission lines in the sample. The values are all close to 1.7 μm, rising to just above 2 μm below 4 keV.

Figure 3 shows a virtual 2D composition map, obtained with confocal XRF at CHESS, of the near-surface region of a grain of dry brown rice [6]. In this case, the 7 μm $\times$ 4 mm channel array was used. Due to its large variety of elemental constituents, the sample serves to illustrate excellent spatial resolution ($d_R = 5$ μm in this case) for low energy emission. The figure shows that the outer surface of the rice grain, or bran, is composed of two layers with distinct composition. Both layers contain potassium, but manganese and phosphorous are selectively distributed in the upper and lower layers, respectively. Since the depth resolution of state-of-the-art, but traditional CXRF implementations generally exceeds 20 μm below 4 keV [2], the potassium and phosphorous concentrations in figure 3 would be severely obscured in CXRF maps of this sample obtained with polycapillaries as the collection optic.

3. Summary

In this article, we have shown that lithographically-defined microchannel arrays constitute a practical and advantageous collection optic for confocal x-ray fluorescence microscopy. Although not shown here, we have also employed these optics for XANES in confocal mode. We anticipate that these optics will significantly enhance and broaden the scope of application of confocal XRF, particularly for light elements and samples with spatial variation on the 1 μm scale.

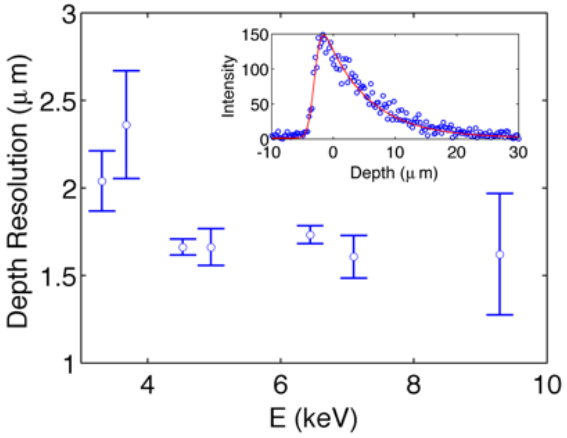

Figure 2. (Color online) Depth resolution $d_R(E)$ for a confocal XRF arrangement employing a channel array with 1 μm$\times$ 4 mm nominal channel dimensions. The inset shows the intensity distribution and fit for potassium Kα, one of the curves employed to obtain $d_R(E)$.

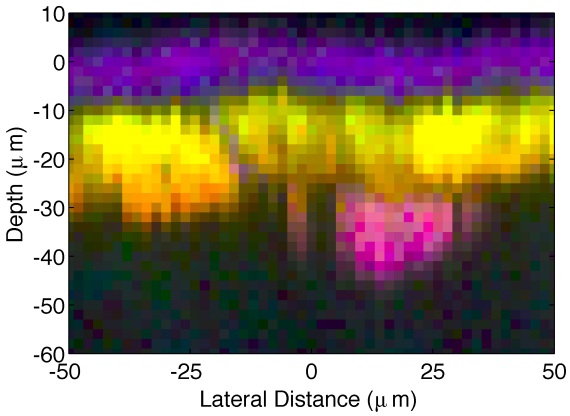

Figure 3. (Color online) Representation of a 2D confocal XRF scan of the the near-surface region of a grain of brown rice. In the image, the Kα intensities of potassium, phosphorus, and manganese are normalized to their maximum, then encoded as red, green, and blue, respectively.

Acknowledgements

This work was supported by the Cornell Center for Materials Research, a National Science Foundation (NSF) Materials Research Science and Engineering Center (NSF-DMR-0520404). This work was performed in part at NSF-supported members of the National Nanotechnology Infrastructure Network, the Lurie Nanofabrication Facility and the Cornell NanoScale Facility(Grant ECCS-0335765). This work was performed in part at the Cornell High Energy Synchrotron Source, supported by the NSF and NIH-NIGMS (NSF-DMR-0225180). PNC/XSD facilities at the Advanced Photon Source, and research at these facilities, are supported by the U.S. Department of Energy - Basic Energy Sciences, a Major Resources Support grant from NSERC, the University of Washington, the Canadian Light Source and the Advanced Photon Source. Use of the Advanced Photon Source, an Office of Science User Facility operated for the U.S. Department of Energy (DOE) Office of Science by Argonne National Laboratory, was supported by the U.S. DOE under Contract No. DE-AC02-06CH11357. JM and ACF acknowledge the Lenfest Foundation for additional support.

References

[1] Kanngießer B, Malzer W, Mantouvalou I, Sokaras D and Karydas A 2011 *Appl. Phys. A: Mat. Sci. and Proc.* 1–14; Perez R D, Sanchez H J, Perez C A and Rubio M 2010 *Radiat. Phys. Chem.* **79** 195–200; Fittschen U E A and Falkenberg G 2011 *Anal. Bioanal. Chem.* **400** 1743–1750

[2] Woll A R, Agyeman-Budu D, Bilderback D H, Dale D, Kazimirov A Y, Pfeifer M, Plautz T, Szebenyi T and Untracht G 2012 *SPIE Optics and Photonics 2012* vol 8502 ed Goto S, Morawe C and Khounsary A M (SPIE) pp 85020K–1 – 85020K–14

[3] Silversmit G, Vekemans B, Appel K, Schmitz S, Schoonjans T, Brenker F E, Kaminsky F and Vincze L 2011 *Anal. Chem.* **83** 6294–6299

[4] Luhl L, Mantouvalou I, Malzer W, Schaumann I, Vogt C, Hahn O and Kanngiesser B 2012 *Anal. Chem.* **84** 1907–1914

[5] Mantouvalou I, Malzer W, Schaumann I, Luhl L, Dargel R, Vogt C and Kanngiesser B 2008 *Anal. Chem.* **80** 819–826

[6] Mihucz V G, Silversmit G, Szalóki I, de Samber B, Schoonjans T, Tatár E, Vincze L, Virág I, Yao J and Záray G 2010 *Food Chemistry* **121** 290 – 297